

Analysis of Deuteron Elastic Scattering in the Framework of the Double Folding Optical Potential ModelM. El-Azab Farid¹, L. Alsagheer², Wedad R. Alharbi² and Awad A. Ibraheem^{3,4}¹Physics Department, Assiut University, Assiut 71516, Egypt²Faculty of Science for Girls, King Abdulaziz University, Jeddah, Saudi Arabia³Physics Department, Al-Azhar University, Assiut Branch, Assiut 71524, Egypt⁴Physics Department, King Khalid University, Abha, Saudia Arabial.alsagheer@gmail.com awad_ah_eb@hotmail.com

Abstract: Deuteron elastic scattering has been analyzed in the framework of the double folding (DF) optical model over the energy range 11.8–171 MeV. Six targets are considered; namely, ¹²C, ¹⁶O, ²⁴Mg, ²⁸Si, ³²S and ⁴⁰Ca. The DF calculations for the real central part of the nuclear optical potential are performed based upon the alpha-nucleon effective interaction. The imaginary part of the optical potential is expressed in a phenomenological Woods-Saxon form. The derived semi microscopic potentials are used to analyze the elastic scattering differential cross section of twenty-five sets of data of the considered systems. Comparisons between the extracted and measured angular distributions of the differential cross sections are presented. A pronounced success to reproduce the data is obtained. [M. El-Azab Farid , L. Alsagheer, Wedad R. Alharbi and Awad A. Ibraheem. **Analysis of Deuteron Elastic Scattering in the Framework of the Double Folding Optical Potential Model.** *Life Sci J* 2014;11(5):208-216]. (ISSN:1097-8135). <http://www.lifesciencesite.com>. 27

Keywords: Optical model, Elastic scattering, Folding potential.

I. Introduction

Investigations of the elastic scattering of nucleons and composite projectiles from nuclei have been studied since the beginning of nuclear physics research. Elastic scattering differential cross sections can be used effectively to extract the projectile-nucleus interaction. The optical model potential (OMP) is the simplest and most successful nuclear model for analyzing scattering processes. Optical potential means a complex potential that represents the interaction between projectile and target nuclei, which when inserted in Schrödinger equation gives reaction cross section and polarization for elastic scattering and some other less important observable quantities. However, a satisfactory semi microscopic or microscopic understanding of the scattering process can be achieved if one relates projectile-target optical potential to the interactions of their constituents through the folding approach by folding.

Deuteron is the simplest (lightest) composite nucleus, so it was natural to study the scattering of this nucleus in terms of the single nucleon. Indeed, it seems a significant concern when Watanabe, before more than fifty years ago[1] analyzed the deuteron nucleus scattering in terms of the potentials of its constituents, proton and neutron. Over the past three decades, several attempts have been made [2-11] for the analysis of deuteron scattering using the nuclear optical potential. All previous analyses(except Ref. 6) were performed using several versions of the phenomenological Woods-Saxon (WS) optical potential.

A microscopic folding calculations were performed by Cook in 1982 [6] to construct double folding (DF) potentials in order to analyze deuteron elastic scattering in the energy range 12-80 MeV and target nuclei in the range $A = 16-208$. The folding procedure was based upon the effective nucleon-nucleon interaction known as M3Y. It was found that it is necessary to reduce the potentials using a normalization factor of ~ 0.87 to obtain agreement between calculated and measured cross sections. So, through the past three decades no other studies have been performed to analyze deuteron scattering using DF potentials.

The present study is devoted to analyze deuteron elastic scattering in the framework of the DF approach. The α -cluster structure of the considered target nuclei is considered in order to perform the DF calculations based upon an effective α -N interaction. The present manuscript is organized as follows: in the next section the theoretical formalism is presented, while procedure is explained in section III. Results and discussion are given in section IV and general conclusions are summarized in section V.

II. Formalism

The deuteron-nucleus interaction is in general expressed as

$$U(R) = -V^{DF}(R) - i[W_0 - 4a_i W_s \frac{d}{dR}]f(R) + V_{Coul}(R) \quad (1)$$

Where R is the relative coordinate between the incident deuteron and the target nucleus, V^{DF} is DF

potential and W_0 is the imaginary potential depth. The imaginary form factor $f(R)$ is usually taken in the phenomenological WS form as

$$f(R) = \left[1 + \exp\left(\frac{R-R_i}{a_i}\right) \right]^{-1} \quad (2)$$

with $R_i = r_i A_T^{1/3}$, A_T is the target mass number. The $V_{Coul}(R)$ is the Coulomb potential, which is adopted to be due to a uniformly charged sphere of radius $R_C = 1.3A_T^{1/3}$ represented as

$$V_{Coul}(R) = \begin{cases} \frac{Ze^2}{2R} \left(3 - \frac{R^2}{R_C^2} \right), & R \leq R_C \\ \frac{Ze^2}{R}, & R \geq R_C \end{cases} \quad (4)$$

where Z is the target atomic number. The real microscopic DF deuteron-nucleus optical potential is derived in the framework of the DF model using the double convolution integral as [12,13]

$$V^{DF}(R) = \int \rho_D(\vec{r}_1) \rho_2(\vec{r}_2) v_{NN}(s) d\vec{r}_1 d\vec{r}_2, \quad s = |\vec{R} - \vec{r}_1 + \vec{r}_2| \quad (5)$$

where $\rho_D(\vec{r}_1)$ and $\rho_2(\vec{r}_2)$ are the nuclear matter density distributions of the deuteron and target, respectively and V_{NN} is the NN interaction.

There are many lines of evidence that nucleons inside the nucleus tend to form clusters [14-22], and the most likely form of these clusters is the α -particle because of its symmetry and high binding energy (28.3 MeV). Considering the α -cluster structure of the target nucleus; i.e, $A_T = 4N_\alpha$, where $N_\alpha = 3, 4, 6, 7, 8$ and 10 for ^{12}C , ^{16}O , ^{24}Mg , ^{28}Si , ^{32}S and ^{40}Ca nuclei, respectively. Then we can express the deuteron-target DF semi microscopic potential based on α -cluster structure of the target nuclei as

$$V^{DF}(R) = \int \rho_D(\vec{r}_1) \rho_C(\vec{r}_2) v_{\alpha N}(s) d\vec{r}_1 d\vec{r}_2, \quad s = |\vec{R} - \vec{r}_1 + \vec{r}_2| \quad (6)$$

Where ρ_C is the α -particle distribution inside the target nucleus and $v_{\alpha N}$ is the alpha-nucleon effective interaction.

The α -N interaction, $V_{\alpha N}$ is considered in the Gaussian form [19,20,23]

$$v_{\alpha N}(s) = v_0 e^{-\eta s^2} \text{ MeV} \quad (7)$$

where $v_0 = 36.4 \text{ MeV}$, $\eta = 0.2657 \text{ fm}^{-2}$

A. Density distributions

The nuclear matter distribution of the deuteron is adopted to have a Gaussian form as [24]

$$\rho_D(r) = \rho_{0D} \exp(-\gamma r^2) \text{ fm}^{-3} \quad (8)$$

where $\rho_{0D} = 0.0992 \text{ fm}^{-3}$, $\gamma = 0.424 \text{ fm}^{-2}$. This density gives a root mean square (rms) radius equals to 1.88 fm which is consistent with that extracted [25] from the high-energy electron-deuteron scattering (1.95 fm).

For the sake of comparison, we use also another version of the deuteron density extracted from the wave function that condone the D-state. Assuming the Hulthen wave function for the S-state formulated as [26]

$$\phi_D(r) = \left[\frac{\alpha\beta(\alpha + \beta)}{2\pi(\alpha - \beta)^2} \right]^{1/2} \frac{e^{-\alpha r} - e^{-\beta r}}{r} \quad (9)$$

where $\alpha = 0.2317 \text{ fm}^{-1}$, $\beta = 6\alpha$. Then, the deuteron density can be derived as

$$\rho_D(r) = 16 |\phi(2r)|^2 \quad (10)$$

This density produce a rms radius equals to 1.93 fm. Figure (1) shows a comparison between the densities (8) and (10). It is noted that the values of nuclear density within the deuteron are equal at 1.0 fm. At the center of the nucleus, the version (10) has an unphysical value and decays rapidly at the surface while the Gaussian one (8) extends to a wider region.

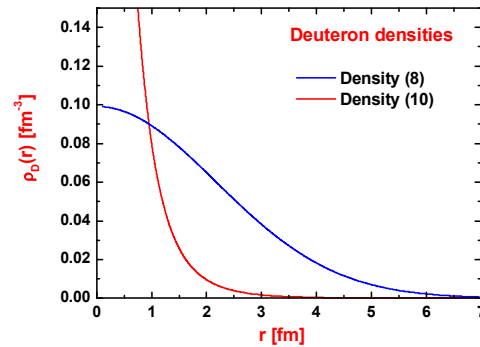


Fig.(1): Comparison between the two nuclear-density distributions (8) and (10).

The α -particle density distributions inside the target nuclei are considered in the harmonic oscillator form [19,20] as

$$\rho_C(r_2) = \rho_{0C} \left[1 + \omega r_2^2 \right] \exp(-\mu r_2^2) \text{ fm}^{-3} \quad (11)$$

The density parameters ρ_{0C} , ω , μ used in the present calculations are given in Ref. [19].

III. Procedure

Calculations are analytically performed to derive the semi microscopic DF potentials (6) for the six targets using both versions of the deuteron matter density (8) and (10). The obtained results showed that both densities lead to similar results, where the difference between each other for all studied nuclei does not exceeds five percent. For this reason, repeating potential calculations by using the density (10) will has no significant value for the study, thus we restrict potential calculations to the Gaussian density (8).

To calculate the elastic scattering cross sections, the derived DF potentials are fed as real parts to the computer program HIOPTM-94 [27] which was programmed based on solving Schrödinger equation. The imaginary part of potential has been considered in the phenomenological WS form (2). The search was carried out on four parameters of imaginary nuclear part in addition to the normalization factor of the real folded potentials, N_R .

Best fits are obtained by minimizing χ^2 , where

$$\chi^2 = \frac{1}{N} \sum_{i=1}^N \left(\frac{\sigma_{th}(\theta_i) - \sigma_{ex}(\theta_i)}{\Delta\sigma_{ex}(\theta_i)} \right)^2. \quad (15)$$

$\sigma_{th}(\sigma_{ex})$ is the theoretical (experimental) cross section at angle θ_i in the c.m. system, $\Delta\sigma_{ex}$ is the experimental error, and N is the number of data points. An average value of 10% is used for the experimental errors of all considered data.

IV. Results and Discussion

The obtained elastic scattering results are shown in comparison with the corresponding measured data in Figs (2-26). The best fit parameters are listed in Table 1. Volume integrals of the real (J_R) and imaginary (J_I) potentials in unit of MeVfm^3 are also shown. Furthermore, the minimum value of χ^2 criterion and the extracted values of absorption

(reaction) cross section, σ_R in unit of mb, are added. For the sake of comparison we present in Figs. (2-26) the results of the complex phenomenological WS potentials reported in Ref. [11].

From these figures, one can note that the deduced semi microscopic DF potentials have

successfully described the angular distributions of the elastic scattering differential cross section all over the measured angular range at all considered energies. In addition, it is evident that the present fits with data are quite better than those obtained in Ref. [11] using complex phenomenological WS potentials, which have more flexibility to fit the data using eleven free parameters. So, the success of present DF potentials produces an additional evidence for the success of the alpha-cluster to describe the structure of the target nuclei.

From Table 1, we find that the behavior of normalization factor N_R with the projectile energy for all used targets does not show a certain behavior by which we can be guided. However, in general, at low energies (less than 100 MeV) N_R is larger than unity, while at large energies (higher than 100 MeV) $N_R < 1$. Also, the results presented on Table 1 prove that there is no feature of the behavior with energy for both real and imaginary volume integrals. The same result can be obtained for the change with the target mass number at a fixed energy. However, the absorption cross-section appeared, as expected, that its value decreases by increasing the energy, and increases by increasing the mass number of target nucleus.

Finally, one can conclude from this study that the semi microscopic optical potentials deduced from the DF model based on the alpha-cluster structure of the target nuclei have quantitatively and qualitatively succeeded in presenting the description of the deuteron elastic scattering at a broad range of energies, 11.8 – 171 MeV.

Table 1: Best fit parameters deduced from analysis of deuteron-target elastic scattering using semi microscopic potentials.

Target	E MeV	N_R	W_0 MeV	W_S MeV	r_1 fm	a_1 fm	$-J_R$ MeVfm^3	$-J_I$ MeVfm^3	χ^2	σ_R mb
^{12}C	11.8	1.76	0.0	12.0	1.683	0.509	652.6	201.6	11.3	1112
	34.4	1.39	0.0	15.9	1.508	0.511	515.5	217.0	0.53	906
	52	1.52	0.0	19.3	1.063	0.730	561.1	225.7	3.52	869
	110	1.16	24.7	0.0	1.456	0.610	412.7	212.5	0.7	627
	170	0.91	29.5	0.0	1.440	0.632	338.0	250.6	3.8	599
^{16}O	11.8	1.39	0.0	9.5	1.650	0.536	516.3	146.0	9.9	1158
	34.4	1.32	0.0	15.8	1.364	0.535	489.5	169.1	3.47	959
	52	1.62	0.0	14.2	1.549	0.586	536.2	214.6	19.8	1045
	56	1.36	0.0	14.4	1.050	0.878	502.0	187.6	5.9	1027
	171	0.86	37.6	0.0	1.159	0.726	318.5	197.5	3.4	625
^{24}Mg	52	1.14	0.0	27.5	0.846	0.887	421.1	214.6	2.01	1206
	56	1.15	0.0	16.3	1.098	0.840	424.4	173.8	10.3	1192
	70	1.21	1.61	25.0	1.440	0.413	448.5	203.6	9.97	1004
	90	1.14	9.36	3.92	1.620	0.655	420.5	162.1	18.4	1095
	170	0.82	8.05	0.0	2.010	0.776	304.4	160.2	10.0	1037
^{28}Si	11.8	1.27	0.0	28.3	1.579	0.435	468.9	259.2	1.5	1237
	52	1.20	0.0	12.8	1.390	0.692	443.6	154.9	20.9	1290
	56	1.17	14.0	0.0	1.714	0.509	432.9	161.4	5.0	1160
^{32}S	11.8	1.20	8.63	6.16	1.760	0.371	442.8	160.1	2.8	1268

⁴⁰ Ca	52	1.09	1.74	13.5	1.272	0.755	404.5	155.8	13.3	1349
	56	1.12	0.684	17.8	1.220	0.670	414.9	157.6	3.9	1237
	171	0.79	13.71	4.4	0.77	1.449	293.2	129.7	13.1	1175
	34.4	1.01	0.0	15.3	1.380	0.584	375.8	131.8	8.7	1388
	56	0.88	8.99	0.0	1.740	0.830	328.1	118.1	1.2	1510
	140	0.65	48.7	0.0	0.988	0.754	241.7	146.7	5.3	904

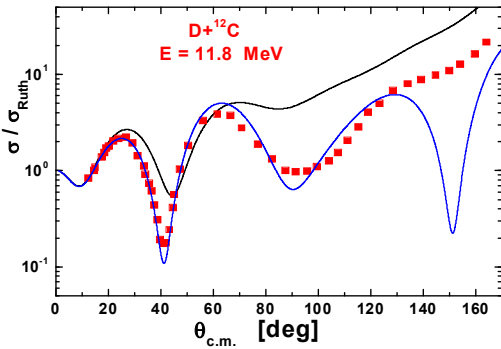


Fig. 2: Angular distribution of $D+^{12}C$ elastic scattering differential cross-section at energy 11.8 MeV using the semimicroscopic potential (9). Blue line is for the present study and the black line is for Ref. [11]. Data are taken from Ref. [28].

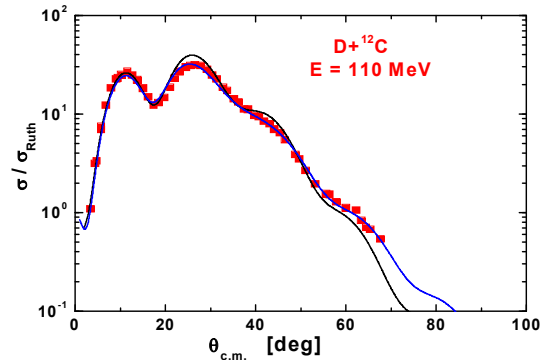


Fig. 5: Same as Fig. 2 but at energy 110 MeV.

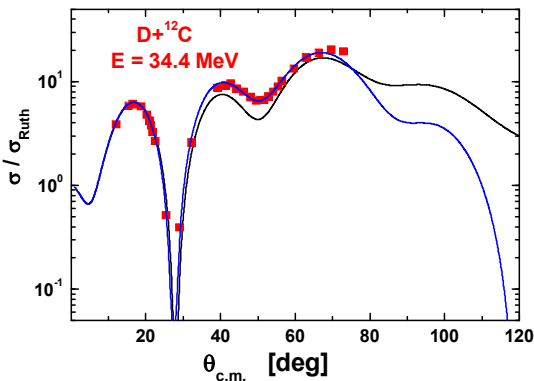


Fig. 3: Same as Fig. 2 but at energy 34.4 MeV.

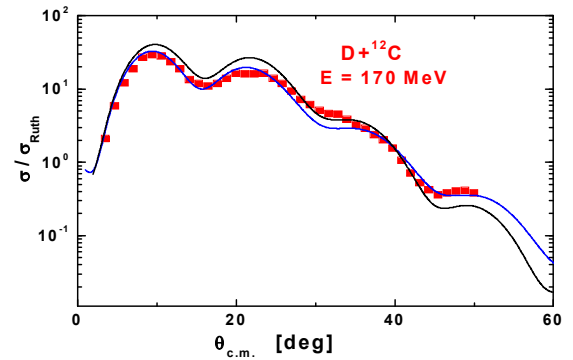


Fig. 6: Same as Fig. 2 but at energy 170 MeV.

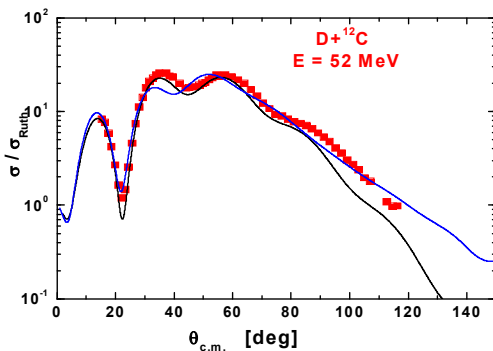


Fig. 4: Same as Fig. 2 but at energy 52 MeV.

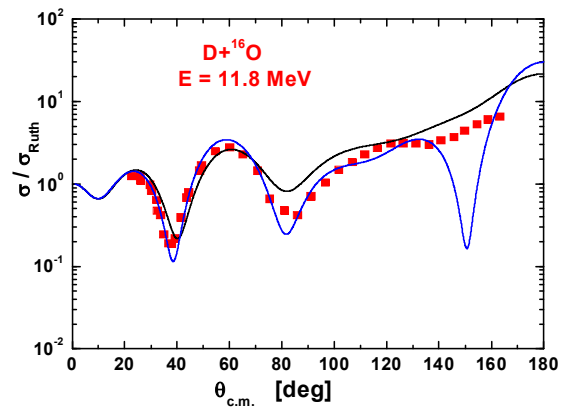


Fig. 7: Same as Fig. 2 but for the $D+^{16}O$ reaction.

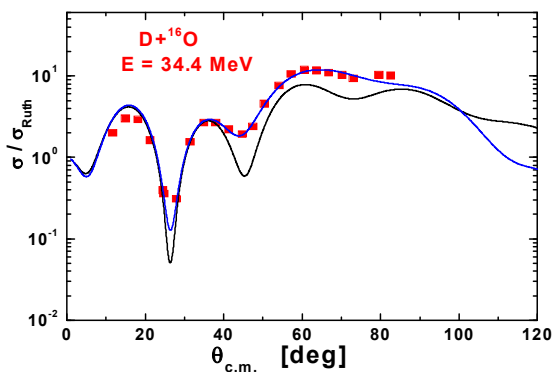


Fig. 8: Same as Fig. 3 but for the $D+^{16}\text{O}$ reaction.

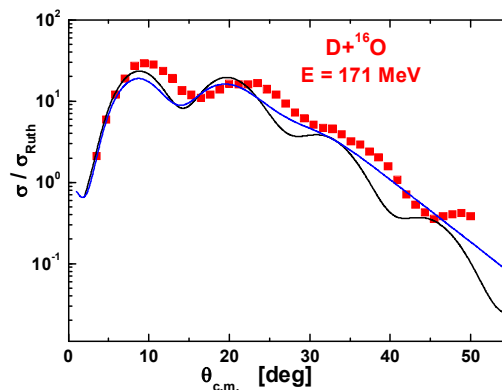


Fig. 11: Same as Fig. 9 but at 171 MeV.

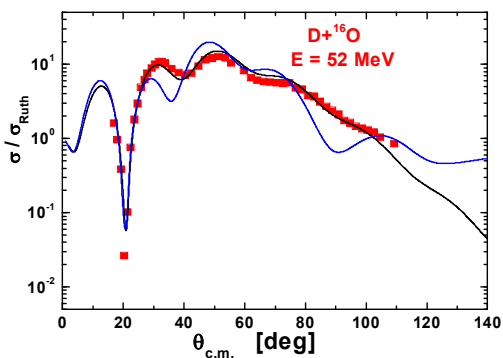


Fig. 9: Same as Fig. 4 but for the $D+^{16}\text{O}$ reaction.

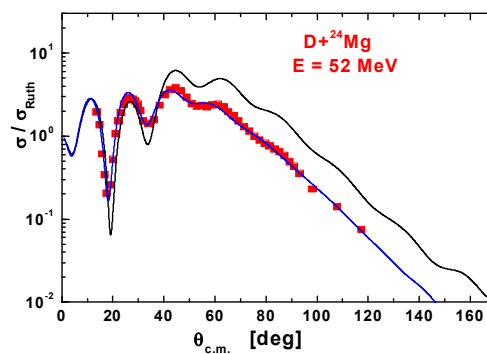


Fig. 12: Same as Fig. 9 but for the $D+^{24}\text{Mg}$ reaction.

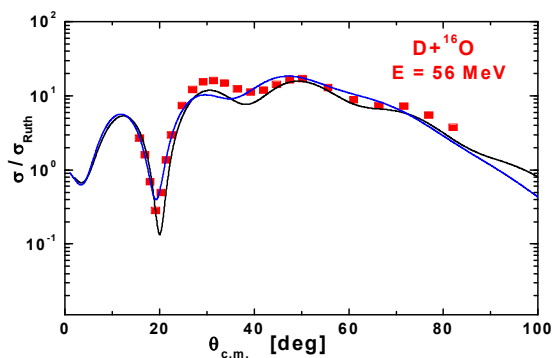


Fig. 10: Same as Fig. 9 but at 56 MeV.

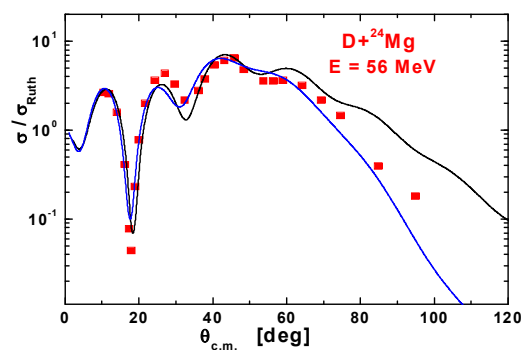


Fig. 13: Same as Fig. 10 but for the $D+^{24}\text{Mg}$ reaction.

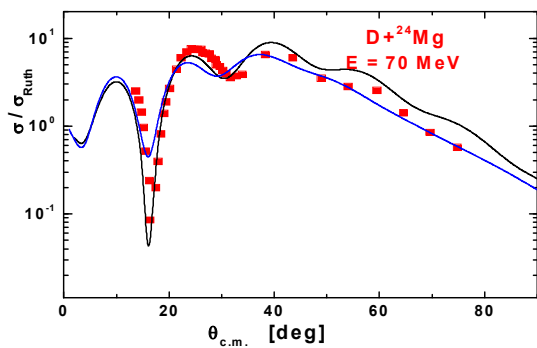


Fig. 14: Same as Fig. 13 but at energy 70 MeV.

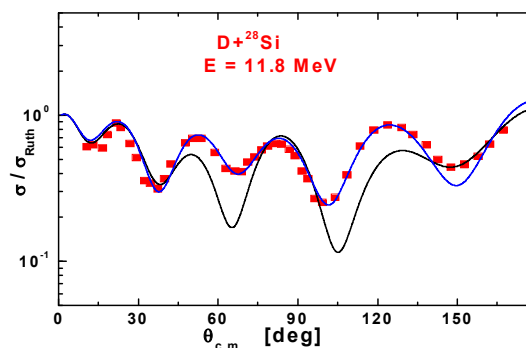


Fig. 17: Same as Fig. 3 but for the $D+^{28}\text{Si}$ reaction.

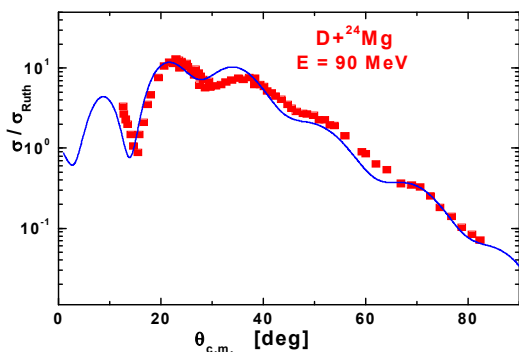


Fig. 15: Same as Fig. 13 but at 90 MeV and potential is available from Ref. [11].

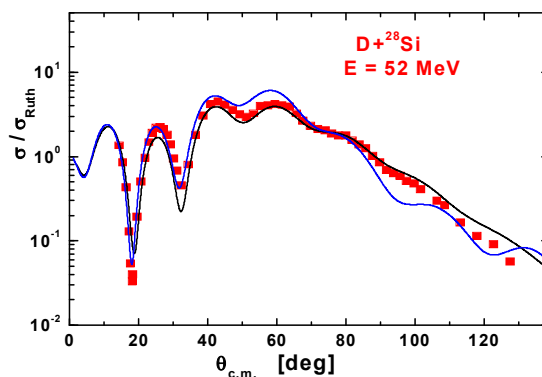


Fig. 18: Same as Fig. 4 but for $D+^{28}\text{Si}$ reaction.

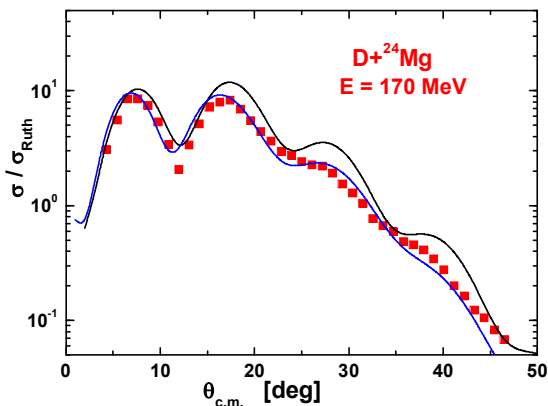


Fig. 16: Same as Fig. 13 but at 170 MeV.

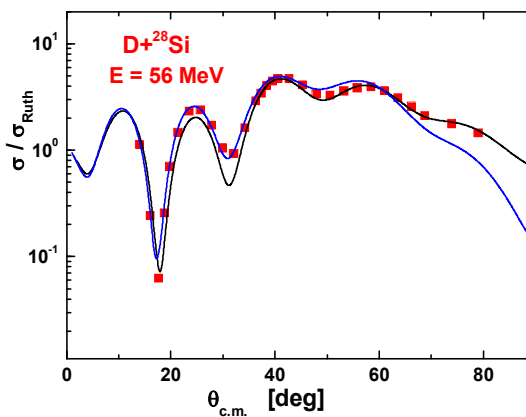


Fig. 19: Same as Fig. 4 but for $D+^{28}\text{Si}$ reaction.

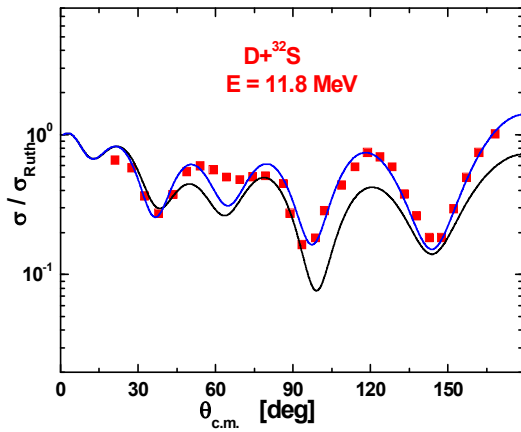


Fig. 20: Same as Fig. 2 but for $D+^{32}\text{S}$ reaction.

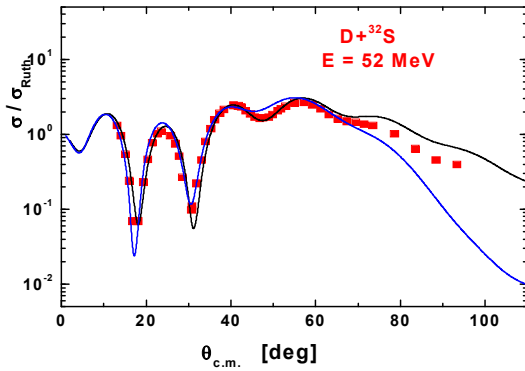


Fig. 21: Same as Fig. 20 but at 52 MeV.

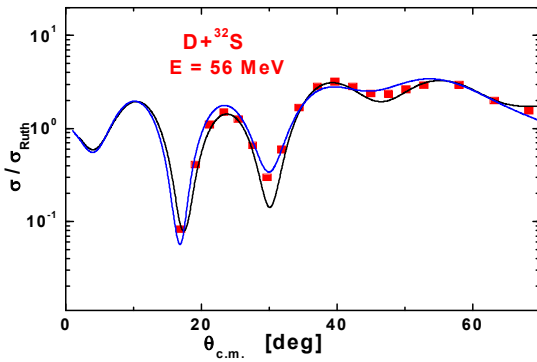


Fig. 22: Same as Fig. 21 but at 56 MeV.

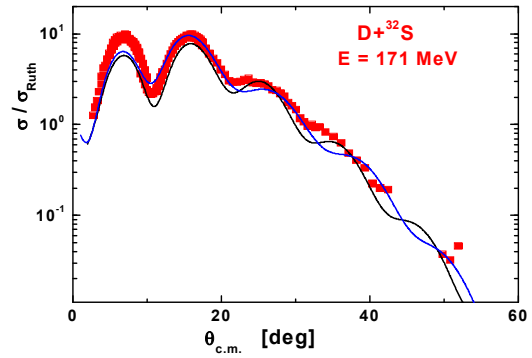


Fig. 23: Same as Fig. 22 but at 171 MeV.

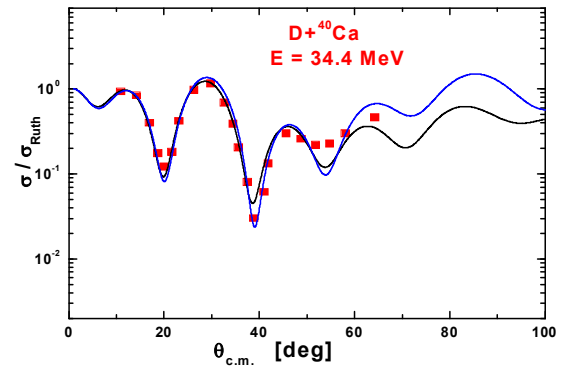


Fig. 24: Same as Fig. 4 but for $D+^{40}\text{Ca}$ reaction.

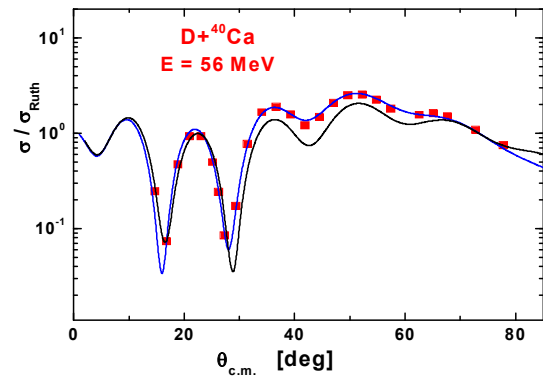


Fig. 25: Same as Fig. 24 but at 56 MeV.

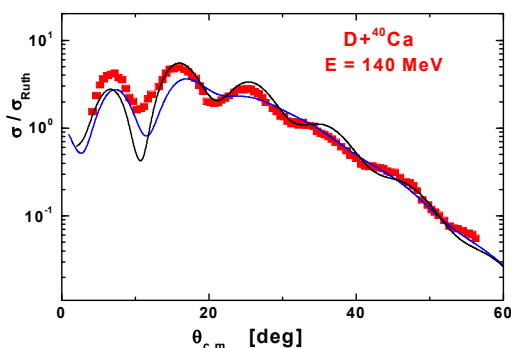


Fig. 26: Same as Fig. 25 but at 140 MeV.

V. Conclusions

The proposed study deals with the analysis of deuteron elastic scattering from different target nuclei which are carbon 12, oxygen 16, magnesium 24, silicon 28, sulfur 32, and calcium 40 at a broad range of energies 11.8 – 171 MeV. The analysis is performed using DF potentials based on the consideration of the alpha-cluster structure of the target nuclei.

Investigating twenty five sets of the scattering data revealed that:

1) The value of real normalization factor increases apparently above unity at low energies, and gradually decreases approaching to unity at high energies then decreases beyond this value by incremental change in projectile energy, indicating that the nuclear potential is deep at low energy and shows its shallowness by increasing the energy.

2) The used model showed an apparent success in describing the elastic scattering reactions for deuteron projectiles with the studied target nuclei which are characterized by the alpha-cluster structure, this success had a significant value at low energies more than at relatively higher energies. This indicates that the tendency of nuclei to form alpha-clusters is a real phenomenon to a considerable extent.

3) The volume integral value of the imaginary potential diminishes at any energy by increasing the mass number of target nucleus.

4) The value of reaction cross-section significantly increases at any energy by progressively increasing the mass of the target nucleus.

5) All imaginary nuclear potentials used in the present studied energies, whether surface or volume forms, reveal significant shallowness, where its maximum depth did not exceed 20 MeV.

6) The success achieved in this study may encourage researchers in the near future to test the derived DF potentials in the analysis of deuteron inelastic scattering data.

References

- [1] Watanabe S., High energy scattering of deuterons by complex nuclei, Nucl. Phys. **8**, 484 (1958).
- [2] Johnson R.C. and P.J.R. Soper, Contribution of Deuteron Breakup Channels to Deuteron Stripping and Elastic, phys. Rev. **C1**, 976 (1970).
- [3] Rawitscher G.H, Effect of deuteron breakup on elastic deuteron - nucleus scattering ,Phys. Rev. **C9**, 2210 (1974); Rawitscher G.H. and S.N. Mukherjee, Second-order breakup corrections to elastic deuteron-nickel scattering between 13 and 80 MeV, Nucl. Phys. **A342**, 90 (1980).
- [4] Farell J.P., C.M. Vincent and N. Austern, T hree-body model of deuteron breakup and stripping, Ann. of Phys. **96**, 333 (1976); Austern N., C.M. Vincent and J.P. Farell, Three-body model of deuteron breakup and stripping, Ann. of Phys. **114**, 93 (1978).
- [5] Amakawa H., S. Yamaji, A. Mori and K. Yazaki, Adiabatic treatment of elastic deuteron-nucleus scattering, Phys. Lett. **B82**, 13 (1979).
- [6] Cook J. Double-folding model analysis of deuteron elastic scattering , Nucl. Phys. **A382**, 61 (1982).
- [7] Van Sen N., J. Arvieux, Y. Yanlin, G. Gaillard, B. Bonin, A. Boudard, G. Bruge, J.C. Lugo, R. Babinet, T. Hasegawa, F. Soga, J.M. Cameron, G.C. Neilson and D.M. Sheppard, Elastic scattering of polarized deuterons from ^{40}Ca and ^{58}Ni at intermediate energies, Phys. Lett. **B156**, 185 (1985).
- [8] Bojowald J., H. Machner, H. Nann, W. Oelert, M. Rogge, and P. Turek, Elastic deuteron scattering and optical model parameters at energies up to 100 MeV, Phys. Rev. **C38**, 1153 (1988).
- [9] A.C. Betker, C.A. Gagliardi, D. R. Semon, R. E. Tribble, H.M. Xu and A.F. Zuruba, Deuteron elastic scattering at 110 and 120 MeV, Phys. Rev. **C48**, 2085 (1993).
- [10] Baumer C., R. Bassini, A.M. van den Berg, D. De Frenne, D. Frekers, M. Hagemann, V.M. Hannen, M.N. Harakeh, J. Heyse, M.A. de Huu, E. Jacobs, M. Mielke, S. Rakers, R. Schmidt, H. Sohlbach and H.J. Wortchel, Deuteron elastic and inelastic scattering from ^{12}C , ^{24}Mg , and ^{58}Ni at 170 MeV , Phys. Rev. **C63**, 037601 (2001).
- [11] An Haixia and C. Cai, Global deuteron

- optical model potential for the energy range up to 183 MeV, Phys. Rev. **C73**, 054605 (2006).
- [12] Satchler G.R. and W.G. Love, Folding model potentials from realistic interactions for heavy-ion scattering, Phys. Rep. **55**, 189 (1979).
- [13] El-Azab Farid M. and G.R. Satchler, A density-dependent interaction in the folding model for heavy-ion potentials, Nucl. Phys. **A438**, 525 (1985); *ibid*, some optical-model analyses of the elastic scattering of ^{40}Ar at 1760 MeV. Nucl. Phys. **A441**, 157 (1985).
- [14] Hodgson P.E., Alpha-clustering in nuclei, Nature **257**, 446 (1975).
- [15] Michel F., α -clustering in the ground state of ^{40}Ca , Phys. Lett. **60B**, 229 (1976).
- [16] Khallaf S.A.E., A.L. Elattar, and M. El-Azab Farid, Elastic scattering of ^{12}C ions using the Watanabe superposition model, J. Phys. G **8**, 1721 (1982).
- [17] Majka Z., H. J. Gils, and H. Rebel, Cluster folding model for $\text{C}^{12}(\text{Li}^6, \text{Li}^6)$ scattering at 156 MeV, Phys. Rev. **C25**, 2996 (1982).
- [18] El-Azab Farid M., Folding models for the elastic scattering of $^7\text{Li}+^{12}\text{C}$, J. Phys. **G15**, 1437 (1989); *ibid*, Four-alpha cluster folding model of ^{16}O -ions, **G16**, 461 (1990).
- [19] El-Azab Farid M., Z.M.M. Mahmoud and G.S. Hassan, Analysis of heavy ions elastic scattering using the double folding cluster model, Nucl. Phys. **A691**, 671 (2001); *ibid*, α -clustering folding model, Phys. Rev. **C64**, 014310 (2001).
- [20] El-Azab Farid M., Heavy ion double folding cluster optical potentials, Phys. Rev. **C65**, 067303 (2002).
- [21] Hassanain M.A., Awad A. Ibraheem and M. El-Azab Farid, Double folding cluster potential for $\text{C}^{12}+\text{C}^{12}$ elastic scattering, Phys. Rev. **C77**, 034601 (2008).
- [22] Hassanain M.A., Awad A. Ibraheem, S.M.M. Al Sebiey, S.R. Mokhtar, M.A. Zaki, Zakaria M.M. Mahmoud, K.O. Behairy and M. El-Azab Farid, Investigation of $^{16}\text{O}+^{16}\text{O}$ elastic scattering using the α -cluster folding model, Phys. Rev. **C87**, 064606 (2013).
- [23] Bertrand F.E., G.R. Satchler, D.J. Horen, J. R. Wu, A.D. Bacher, G.T. Emery, W.P. Jones, D.W. Miller and A. van der Woude, Giant multiple resonances from inelastic scattering of 152-MeV alpha particles, Phys. Rev. **C 22**, 1832 (1980).
- [24] Abul-Magd A.Y. and M. El-Nadi, Optical Model Parameters for Composite Particles, Prog. Theor. Phys. **35**, 798 (1966);
- [25] Keaton P.W., E. Aufdembrink and L.R. Vesser, Los Laboratory Report LA-4379-MS (1969) (unpublished).
- [26] Allen L.J., J.P. McTavish, M.W. Kermode and A. McKerrell, The root-mean-square radius of the deuteron, J. Phys. **G7**, 1367 (1981).
- [27] Clarke N.M., An optical model search program (1994) (unpublished).
- [28] www.nndc.bnl.gov/exfor/exfor000.htm.

3/11/2014